Phase behavior and rheology of attractive rod-like particles

Fei Huang,[a] Roy Rotstein,[a] Seth Fraden,*[a] Karen E. Kasza[b] and Nolan T. Flynn[c]

Received 6th January 2009, Accepted 3rd April 2009
First published as an Advance Article on the web 13th May 2009
DOI: 10.1039/b823522h

Colloidal rods interacting with a temperature-dependant attraction are constructed by grafting the polymer poly(*N*-isopropylacrylamide) (PNIPAM) to the surface of the charged, semi-flexible filamentous fd virus. The phase diagram of fd-PNIPAM system becomes independent of ionic strength at high salt concentration and low temperature, *i.e.*, the rods are sterically stabilized by the polymer. However, the network of rods undergoes a sol–gel transition as the temperature is raised. The viscoelastic moduli of fd and fd-PNIPAM suspensions are compared as a function of temperature, and the effect of ionic strength on the gelling behavior of fd-PNIPAM solution is measured. For all fluid-like and solid-like samples, the frequency-dependant linear viscoelastic moduli can be scaled onto universal master curves.

1 Introduction

The phase behavior of a fluid of rod-like particles interacting through short range repulsion has been well described at the second virial coefficient level by Onsager[1] who demonstrated that this system exhibits an isotropic–nematic (*I–N*) phase transition. Examples of colloidal liquid crystals range from minerals[2] to viruses,[3] with theory agreeing with experimental results in many cases. Attempts have been made to explore the influence of attractive interactions on the *I–N* transition both theoretically and experimentally. One approach to introduce attractions has been through "depletion attraction"[4] in which rods and polymers are mixed resulting in an attractive potential of mean force. Several theoretical works have incorporated depletion attraction into the Onsager theory[5,6] and a simulation has also been performed.[7] These studies predict a widening of the biphasic *I–N* gap. These results are in qualitative agreement with the measured *I–N* transition in mixtures of boehmite rods and polystyrene polymers and mixtures of charged semiflexible fd virus and dextran polymers.[8–10] For the case of direct interparticle attraction, theory also predicts that the width of the *I–N* coexistence widens abruptly with increasing attraction.[11,12] However, in experiments with the semiflexible polymer, PBG, experiments show that a gel phase supersedes the *I–N*.[13]

In this work, we consider the effect of direct attractions on the phase behavior of colloidal rod-like particles. As a model colloidal rod we use aqueous suspensions of filamentous semiflexible bacteriophage fd. Suspensions of fd have been previously shown to exhibit an *I–N* transition in agreement with theoretical predictions for semiflexible rods interacting with a salt dependent effective hard rod diameter D_{eff}.[14] Although fd forms a cholesteric phase, the difference in free energy between the cholesteric and nematic phases is much smaller than that between the isotropic and nematic phases. Hence we refer to the cholesteric phase as the nematic phase in this paper.

We have developed a temperature sensitive aqueous suspension of colloidal rods. Specifically, thermosensitive poly(*N*-isopropylacrylamide) polymers (PNIPAM) are covalently linked to the virus major coat protein pVIII. Solutions of PNIPAM have a lower critical solution temperature (LCST) in water. Below its LCST of 32 °C, PNIPAM is readily soluble in water, while above its LCST the polymer sheds much of its bound water and becomes hydrophobic, which leads to collapse of the coil, attraction between polymers, and phase separation.[15,16] The fd virus has been shown to have a robust thermal stability up to 90 °C.[17] Previously, mixtures of fd and PNIPAM have been used to investigate melting of lamellar phases.[18] Here we explore the behavior of suspensions of fd-PNIPAM particles as a function of temperature. A reversible sol–gel transition is found for both the isotropic and nematic phase and is studied in detail with dynamic light scattering (DLS) and rheometry. As the system can be driven reversibly from a fluidic state to a gel state, fd-PNIPAM suspensions are a versatile model system to study the fundamental properties of entangled and crosslinked networks of semiflexible polymers.

2 Materials and methods

2.1 Preparation of fd-PNIPAM complexes

Bacteriophage fd is a rodlike semiflexible polymer of length $L = 880$ nm, diameter $D = 6.6$ nm, molecular weight 1.64×10^7 dalton, surface charge density $7e^-$/nm at pH = 8.2 and has a persistence length between 1 and 2 μm.[19,20] There are approximately 2700 major coat proteins helically wrapped around the phage genome of a single-stranded DNA. The fd virus is grown and purified as described elsewhere.[21] The virus concentration is determined by UV absorption at 269 nm using an extinction coefficient of 3.84 cm^2/mg on a spectrophotometer (Cary-50, Varian, Palo Alto, CA, USA).

About 30 mg NHS-terminated PNIPAM with a molecular weight of 10 000 g/mol (Polymer Source Inc., Quebec, Canada) is mixed with 800 μl of 24 mg/ml fd solution for 1 h in 20 mM phosphate buffer at pH = 8.0. The reaction product is centrifuged repeatedly to remove the excess polymers. The PNIPAM-bound

[a]*Department of Physics, Brandeis University, Waltham, MA, 02454, USA*
[b]*Department of Physics & DEAS, Harvard University, Cambridge, MA, 02138, USA*
[c]*Department of Chemistry, Wellesley College, Wellesley, MA, 02481, USA*

fd virus is stored in 5 mM phosphate buffer at 4 °C for future use. Using a differential refractometer (Brookhaven Instruments, Holtsville, NY, USA) at $\lambda = 620$ nm, the refractive index increment, (dn/dc), is measured to estimate the degree of polymer coverage of the fd virus.[22] There are 336 ± 60 polymer chains grafted on each virus, which corresponds to a grafting density of $N/\pi DL = 0.02$ PNIPAM/nm^2, a nearly complete coverage of the rod by the polymer.

2.2 Dynamic light scattering

In a homodyne light scattering experiment, the time correlation function of the scattered light intensity is acquired,

$$G_I(q,t) = \frac{\langle I(q,0)I(q,t)\rangle}{\langle I(q)\rangle^2} \quad (1)$$

This can be related to the correlation function of the electric field by the Siegert relation,[23]

$$G_E(q,t) = \sqrt{G_I(q,t)^2 - 1} \quad (2)$$

where

$$G_E(q,t) = \frac{\langle E^*(q,0)E(q,t)\rangle}{\langle I(q,t)\rangle} \quad (3)$$

An effective diffusion coefficient can be defined by the first cumulant

$$D_{\text{eff}}(q) = \Gamma(q)/q^2 \quad (4)$$

where

$$\Gamma = -\frac{\mathrm{d}}{\mathrm{d}t}[\ln G_E(q,t)]_{t\to 0} \quad (5)$$

Here the $D_{\text{eff}}(q)$ reflects the different types of motion associated with the rod-like fd-PNIPAM particle, including translation, rotation and bending motion.

A light scattering apparatus (ALV, Langen, Germany) consisting of a computer controlled goniometer table with focusing and detector optics, a power stabilized 22 mW HeNe laser (λ = 633 nm), and an avalanche photodiode detector connected to an 8 × 8 bit multiple tau digital correlator with 288 channels was used to measure the correlation function. The temperature of the sample cell in the goniometer system is controlled to within ±0.1 °C.

To remove dust and air bubbles in the fd-PNIPAM solution, the sample was passed through a 0.45 μm filter and centrifuged at 3000 rpm for 15 min before each measurement. The correlation function of the scattered light intensity was measured at a scattering angle of 90°. The particle concentration ranges from $2c^*$ to $4c^*$ with the critical concentration $c^* = 1$ particle/L^3 or 0.04 mg/ml.

2.3 Rheological characterization of fd-PNIPAM suspensions

The rheological measurements were carried out on a stress-controlled rheometer (TA Instruments, New Castle, DE, USA) using a stainless steel cone/plate tool (2° cone angle, 20 mm cone diameter). The gap is set at 70 μm at the center of the tool. The torque range is 3 nN·m to 200 mN·m, and the torque resolution is 0.1 nN·m. The temperature control is achieved by using a Peltier plate, with a range of −20 °C to 200 °C and an accuracy of ±0.1 °C.

The storage and loss moduli, $G'(\omega)$ and $G''(\omega)$, respectively, are measured as a function of frequency by applying a small amplitude oscillatory stress at a strain amplitude $\gamma = 0.03$. A strain sweep is conducted prior to the frequency sweep to ensure the operation is within the linear viscoelastic regime.

3 Results and discussion

Onsager[1] first predicted that there is an *I*–*N* phase transition in suspensions of hard rods when the number density of rods c reaches $\frac{1}{4}c\pi L^2 D = 4$, where L and D are the length and diameter of the rods, respectively. Since the fd virus is charged, it is necessary to account for the electrostatic repulsion by substituting the bare diameter D with an effective diameter D_{eff}, which is larger than D by an amount roughly proportional to the Debye screening length. As the solution ionic strength increases, D_{eff} decreases and eventually approaches D. Fig. 1 presents the *I*–*N* coexisting concentrations, c, as a function of ionic strength for fd,[14] showing that c rises with increasing ionic strength and, in fact, $c \propto 1/D_{\text{eff}}$. Fig. 1 also shows coexistence concentrations for fd to which different polymers (PEG,[24] PNIPAM) have been covalently grafted to its surface. The polymer grafted particles are denoted as fd-PEG[24] and fd-PNIPAM, respectively. All measurements are made at room temperature under conditions for which water is a good solvent for both the PEG and PNIPAM polymers. The *I*–*N* coexistence concentrations of both fd-PEG and fd-PNIPAM are independent of ionic strength at high ionic strength. The physical picture is that the electrostatic effective diameter D_{eff} decreases with increasing ionic strength. However, there is also a diameter associated with the polymer diameter, D_{poly}, which is independent of ionic strength (at least for the range of salt concentration in this experiment). Once D_{eff}

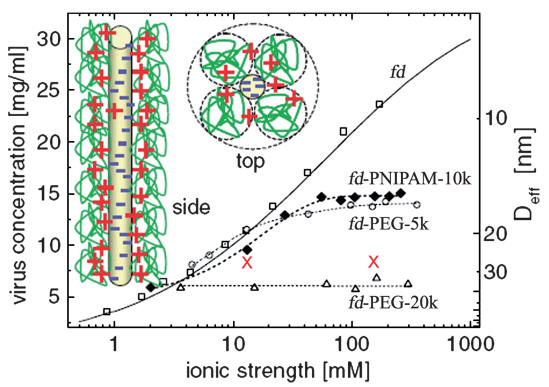

Fig. 1 (Color in online version) Isotropic-nematic coexistence concentration of PNIPAM-coated fd virus as a function of ionic strength (solid symbol). The lines indicate the highest concentration for which the isotropic phase is stable. Plotted in addition for comparison is data on wild-type fd, fd-PEG-5k and fd-PEG-20k.[24] As the salt concentration increases, the fd-PNIPAM system transitions from an electrostatically-stabilized suspension to a sterically-stabilized suspension. This is schematically demonstrated by the cartoon of fd-PNIPAM particle with $D^{\text{electrostatic}}_{\text{eff}} < D^{\text{polymer}}_{\text{eff}}$. The cross symbol denotes two conditions for which the rheological properties of fd-PNIPAM were measured.

$< D + 2D_{poly}$ the interparticle interactions are dominated by steric repulsion of the grafted polymer and not electrostatic repulsion. For fd-PNIPAM the transition from electrostatic to polymer stabilized interactions occurs at $D_{eff} \sim 17$ nm. Since the bare fd diameter $D = 7$ nm, the grafted PNIPAM has a corresponding diameter $D_{poly} = 5$ nm, which is comparable to the literature value of the diameter of gyration of PNIPAM in dilute solute of $D_g = 6.4$ nm.[25]

We study the phase behavior of fd-PNIPAM in response to temperature changes. We prepare samples in the isotropic (9.6 mg/ml) and nematic (21 mg/ml) phases at an ionic strength $I =$ 155 mM. At room temperature, both isotropic and nematic samples are transparent viscous fluids. The nematic sample exhibits birefringence under cross polarizers, whereas the isotropic sample does not. As the temperature is increased to $T =$ 40 °C, the samples rapidly turn into viscoelastic gels. These behaviors can be observed by simply tilting the vial, and observing the formation of a weight-bearing gel. As the temperature returns to room temperature, the samples flow like fluids again. The entire process can be repeated multiple times, which indicates a reversible sol–gel transition. This observation can be interpreted as the result of increased hydrophobic attraction among monomers along the PNIPAM chain leading to the collapse of PNIPAM coils into globules at elevated temperature and thus leading to an attraction between the fd-PNIPAM rods.[26]

We load the above mentioned samples into glass capillaries that are subsequently sealed with flame. The samples are placed in a heated block at 40 °C, and monitored with polarizing microscopy for up to a week. No phase separation was observed for either the isotropic or nematic samples, which remain in their respective phases. This is qualitatively different from theory, which predicts that increased attraction leads to enhanced phase separation.[6,11,12] We speculate that the "sticky" rods at high temperature could be kinetically arrested in a non-equilibrium state and therefore do not phase separate during the course of the experiment. As shown in Fig. 2, an increase of temperature, or equivalent attraction, did not induce the solution of rods to phase separate. Instead, with increasing temperature, a gel phase forms at a temperature that is presumably below that at which the phase diagram opens up into a dense nematic coexisting with a dilute isotropic.

We employ rheometry to characterize the gelation of the fd-PNIPAM suspension. Fig. 3 shows $G'(\omega)$ and $G''(\omega)$ for bare fd and fd-PNIPAM solutions measured at two different temperatures. Temperature change has little effect on the storage and loss moduli of the bare fd suspension. By fitting the data to a power law, we have for fd $G'(\omega) \propto \omega^{0.9}$ and $G''(\omega) \propto \omega^{0.7}$. The frequency exponents are consistent with those measured with microrheology.[27] In contrast, fd-PNIPAM becomes solid-like at 38 °C with G' about five times greater than G''. The linear moduli are nearly independent of frequency: $G'(\omega) \propto \omega^{0.14}$ and $G''(\omega) \propto \omega^{0.05}$.

We investigate the effect of ionic strength on the gelation of the fd-PNIPAM network. Fig. 4 illustrates the frequency-dependent viscoelastic moduli as a function of temperature. Parts (a) and (b) represent data taken near the gel point $T = T_c$ from samples under low and high salt conditions, respectively. For $T < T_c$, the suspension shows characteristics typical of a viscous fluid. The gel point is identified as the temperature at which $G'(\omega)$ and $G''(\omega)$ assume the same power law dependence on oscillation frequency.[28] As the temperature increases beyond $T = T_c$, both $G'(\omega)$ and $G''(\omega)$ increase dramatically for the fd-PNIPAM sample and the suspension is clearly gel-like with $G'(\omega)$ weakly dependent on ω.

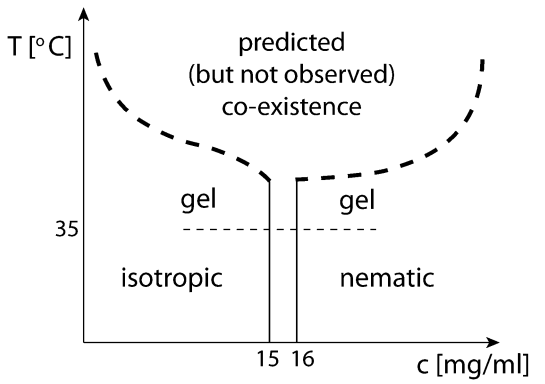

Fig. 2 Predicted phase diagram for attractive fd-PNIPAM at 155 mM ionic strength.[11,12] The solid and light dashed lines indicate what is observed, a narrow isotropic-nematic coexistence that does not vary with temperature. Above 35 °C the samples gel irrespective of phase. The heavy dash line indicates what we expect qualitatively but did not observe, a sudden widening of coexistence region with increased attraction between rods.

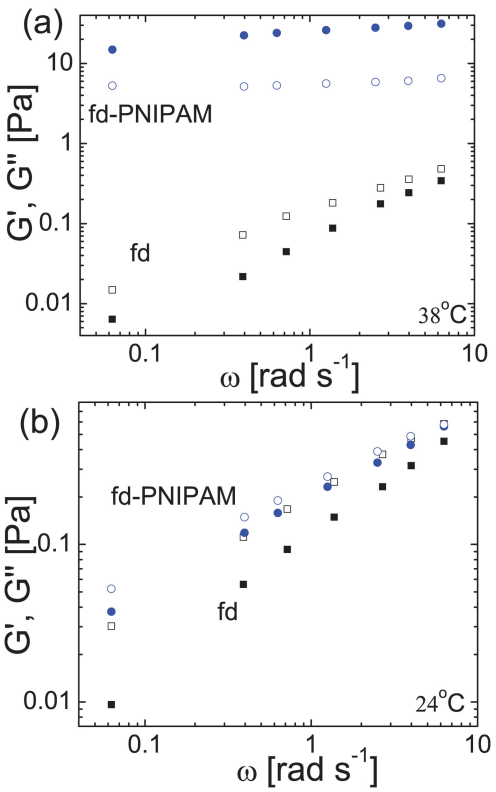

Fig. 3 Storage modulus (solid symbol) and loss modulus (open symbol) of fd (squares) and fd-PNIPAM (circles) suspensions at two different temperatures. (a) $T = 38$ °C, (b) $T = 24$ °C. The concentration of the samples are about 8 mg/ml. The solution ionic strength is 155 mM.

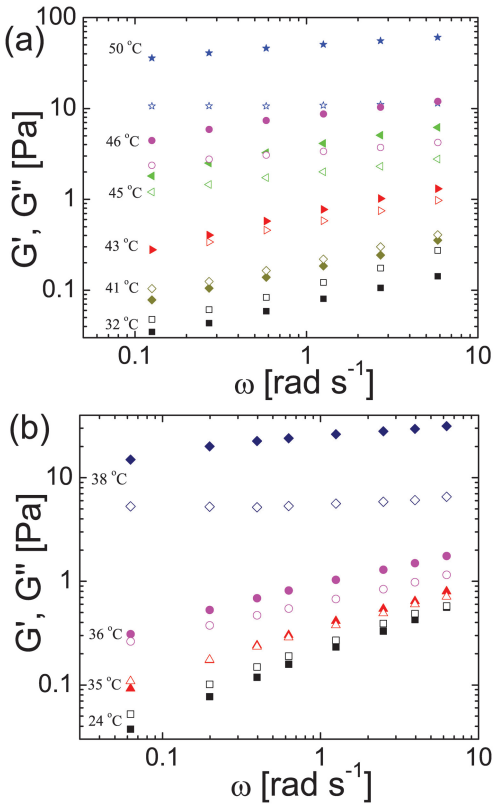

Fig. 4 Storage modulus (solid symbol) and loss modulus (open symbol) of fd-PNIPAM solution as a function of temperature. Ionic strength $I =$ (a) 13 mM, (b) 155 mM. The concentration of the samples are about 8 mg/ml.

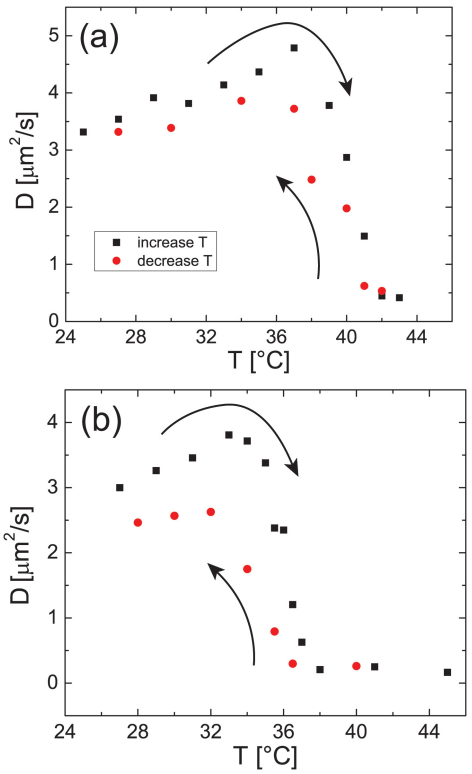

Fig. 5 Diffusion coefficients of fd-PNIPAM at 0.15 mg/ml as functions of temperature. Ionic strength $I =$ (a) 13 mM, (b) 155 mM. These values are determined from the first cumulant of $G_E(q, t)$ using eqn (4).

The data in Fig. 4 shows the high and low salt suspensions reach the gel point at different temperatures with the same power law slope. The sample at low ionic strength solidifies at $T_c = 41$ °C, which is significantly greater than the 35 °C gelling temperature for the sample at high ionic strength. However, both suspensions exhibit the same power law exponent $n = 0.40 \pm 0.02$ at the gel point.

As a check for the gel point, dynamic light scattering is performed on the fd-PNIPAM suspensions as shown in Fig. 5. The onsets of aggregation for the low and high ionic strengths occur at 41 °C and 36 °C, respectively. Gelation occurs at the same temperatures as determined by light scattering and rheology. This ionic strength dependence of the gelation temperature arises from the fact that lowering solution ionic strength increases the electrostatic repulsion between the rods, and therefore a larger attraction from the PNIPAM is required to induce aggregation. The influence of ionic strength on the LCST of PNIPAM is rather small in the concentration range of monovalent salt used in this study,[29] therefore it is not considered here.

A recent study by Zhang *et al.*[30] reports an investigation of aqueous solutions of fd-PNIPAM with comparable grafting density and molecular weights of polymers to this study. The *I*–*N* coexistence concentration and the gelling temperature obtained in the above paper are close to our results. Zhang *et al.* characterized the structure of the nematic gel, whereas we focus on the viscoelasticity of fd-PNIPAM solution in the isotropic phase.

To test the reversibility of the temperature-induced sol–gel transition, measurements are carried out on G' at a constant frequency of 1 Hz with increasing and decreasing temperature (Fig. 6). A slight hysteresis is found during the temperature sweep.

The storage and loss moduli curves at different temperatures can be scaled onto master curves. Through a procedure called time-temperature superposition,[31] the frequency dependent G' and G'' curves measured at different temperatures can be

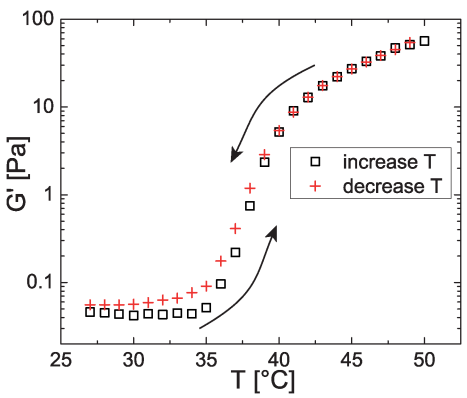

Fig. 6 Reversibility of temperature-induced sol–gel transition. Measurements are made for fd-PNIPAM suspension at 8.4 mg/ml and $I = 13$ mM with increasing and decreasing temperature. The sample is oscillatorally probed at 1 Hz and the rate of temperature change is approximately 1 °C/10 min in both directions.

superposed by shifting along the logarithmic frequency and modulus axes. Specifically we shift data at lower temperatures towards lower frequencies with respect to data at higher temperatures. Time-temperature superposition enables one to probe viscoelasticity for a much larger frequency range than that experimentally accessible. The master curve as shown in Fig. 7(A) reveals that fd-PNIPAM suspensions behave as a thermo-rheologically simple fluid, which means a variation in temperature corresponds to a shift in time scale.[31] The rheological behaviors of fd-PNIPAM are reminiscent of those of polymer melts.[32] At high frequencies, or times shorter than the repetition time, melts behave as solids, while at low frequency the melt can flow. In Fig. 7, similar behavior is observed. At high frequency, which corresponds to high temperature, G' approaches a plateau value and is much larger than G''; thus the material behaves as a solid. In the low frequency limit, the suspension behaves more like a fluid. G' and G'' cross at an intermediate frequency with the slope of G'' equal to 0.36. The temperature-dependent shift factors are plotted in Fig. 7(B). Notably, the frequency shift factor exhibits a break of slope, signifying a phase transition, whereas there is only a minor shift along the logarithmic modulus axis.

Materials that are solid-like at high frequency and liquid-like at low frequency are thixotropic.[33] This is in stark contrast to colloidal gels of precipitated silica particles,[34] carbon nanotubes,[35–37] and carbon black,[38] whose fractal-like microscopic structure leads to the opposite rheological behavior; fluid-like at high frequency and solid-like at low frequency. We hypothesize that the difference in rheological properties between the colloidal gels and our attractive rods is in the nature of the contact between the particles. For bare colloids, such as silica, the interparticle bond is rigid, whereas for the fd-PNIPAM the contact is between two polymers and the interaction is the same as in a polymer melt. At the long time scale of the rheological observation, grafted polymers from one rod that are in contact with those on another rod can sufficiently rearrange their configurations allowing the rods to move with respect to each other, and therefore the suspension flows like a viscous liquid. On a shorter time scale, the polymers are unable to relax and thus the network of rods behaves like a soft solid.

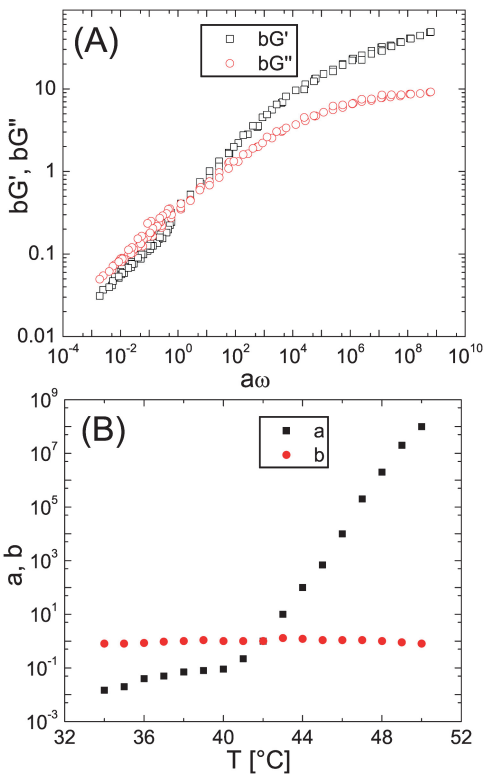

Fig. 7 (A) Master curve showing scaled moduli as functions of scaled frequency. (B) Relationship between shift factors and temperature. a: frequency shift factor. b: modulus shift factor.

For practical applications it may be desirable to create nematic gels of sticky rods such as carbon nanotubes or biological filaments. The implication of our work is that the system has to be repulsively stabilized in order for a nematic to form, in spite of what is predicted theoretically. This is because a gel phase supersedes the *I–N* coexistence as attraction is increased. In the case that a nematic gel is desired, one approach would be to start with a repulsion dominated nematic, such as the low temperature fd-PNIPAM nematic in our work, and then increase attraction so that a nematic gel is formed.

4 Conclusion

We have presented studies of a system of colloidal rods (fd) coated with the temperature-sensitive polymer PNIPAM. At room temperature and high ionic strength, quantitative measurements of the *I–N* transition show fd-PNIPAM behaves as a sterically stabilized suspension. An increase in temperature, or equivalently, strength of attraction, does not lead to a widening of the coexistence concentration as expected. Instead a sol–gel transition arises, which we attribute to the collapse of the grafted PNIPAM polymers. Since gels supersede the *I–N* for both fd-PNIPAM and PBG, an interesting question is whether this is true for all attractive rod systems. Dynamic light scattering and rheometry demonstrate that the gelling process is reversible and ionic strength dependant. Furthermore, the rheological master curves for samples of different temperatures show that the fd-PNIPAM suspensions are rheologically similar to simple polymeric melts.

5 Acknowledgement

We thank D. A. Weitz, N. J. Wagner and Y. Hu for helpful discussions. Financial support of this work comes from NSF (DMR-0444172) and NSF-MRSEC (DMR-0820492).

References

1 L. Onsager, *Ann. N. Y. Acad. Sci.*, 1949, **51**(4), 627.
2 P. Davidson and J. C. P. Gabriel, *Curr. Opin. Colloid Interface Sci.*, 2005, **9**(6), 377.
3 Z. Dogic and S. Fraden, *Curr. Opin. Colloid Interface Sci.*, 2006, **11**(1), 47.
4 S. Asakura and F. Oosawa, *J. Polym. Sci.*, 1958, **33**(126), 183.
5 P. B. Warren, *J. Phys. I*, 1994, **4**(2), 237.
6 H. N. W. Lekkerkerker and A. Stroobants, *Nuovo Cimento D*, 1994, **16**(8), 949.
7 P. G. Bolhuis, A. Stroobants, D. Frenkel and H. N. W. Lekkerkerker, *J. Chem. Phys.*, 1997, **107**(5), 1551.

8 J. Buitenhuis, L. N. Donselaar, P. A. Buining, A. Stroobants and H. N. W. Lekkerkerker, *J. Colloid Interface Sci.*, 1995, **175**(1), 46.
9 M. P. B. van Bruggen and H. N. W. Lekkerkerker, *Macromolecules*, 2000, **33**(15), 5532.
10 Z. Dogic, K. Purdy, E. Grelet, M. Adams and S. Fraden, *Phys. Rev. E*, 2004, **69**(5, Part 1).
11 P. J. Flory, *Proc. R. Soc. London, Ser. A*, 1956, **234**(1196), 73.
12 A. N. Semenov and A. R. Khokhlov, *Sov. Phys. Usp.*, 1988, **31**(3), 988.
13 W. G. Miller, C. C. Wu, E. L. Wee, G. L. Santee, J. H. Rai and K. G. Goebel, *Pure Appl. Chem.*, 1974, **38**(1–2), 37.
14 J. X. Tang and S. Fraden, *Liq. Cryst.*, 1995, **19**, 459.
15 P. G. de Gennes, *Scaling Concepts In Polymer Physics*, Cornell University Press, Ithaca, New York, 1979.
16 H. G. Schild, *Prog. Polym. Sci.*, 1992, **17**(2), 163.
17 Q. Wen and J. X. Tang, *Phys. Rev. Lett.*, 2006, **97**(4), 048101.
18 A. M. Alsayed, Z. Dogic and A. G. Yodh, *Phys. Rev. Lett.*, 2004, **93**(5), 057801.
19 S. Fraden, in *Observation, Prediction, and Simulation of Phase Transitions in Complex Fluids*, ed. M. Baus, L. F. Rull, and J. P. Ryckaert, Kluwer Academic, Dordrecht, 1995.
20 A. S. Khalil, J. M. Ferrer, R. R. Brau, S. T. Kottmann, C. J. Noren, M. J. Lang and A. M. Belcher, *Proc. Natl. Acad. Sci. U. S. A.*, 2007, **104**(12), 4892.
21 T. Maniatis, J. Sambrook, and E. F. Fritsch, *Molecular Cloning: A Laboratory Manual*, Cold Spring Harbor Laboratory Press, Plainview, NY, 2nd edn, 1989.
22 E. Grelet and S. Fraden, *Phys. Rev. Lett.*, 2003, **90**(19), 198302.
23 J. B. Berne and R. Pecora, *Dynamic Light Scattering*, Wiley, New York, 1976.
24 Z. Dogic and S. Fraden, *Philos. Trans. R. Soc. London, Ser. A*, 2001, **359**(1782), 997.
25 K. Kubota, S. Fujishige and I. Ando, *Polym. J.*, 1990, **22**(1), 15.
26 S. Fujishige, K. Kubota and I. Ando, *J. Phys. Chem.*, 1989, **93**(8), 3311.
27 F. G. Schmidt, B. Hinner, E. Sackmann and J. X. Tang, *Phys. Rev. E*, 2000, **62**(4, Part B), 5509.
28 H. H. Winter and F. Chambon, *J. Rheol.*, 1986, **30**(2), 367.
29 Y. J. Zhang, S. Furyk, D. E. Bergbreiter and P. S. Cremer, *J. Am. Chem. Soc.*, 2005, **127**(41), 14505.
30 Z. Zhang, N. Krishna, M. P. Lettinga, J. Vermant and E. Grelet, to be published in Langmuir.
31 J. D. Ferry, *Viscoelastic Properties of Polymers*, Wiley, New York, 3rd edn, 1980.
32 H. M. Laun, *Rheol. Acta*, 1978, **17**(1), 1.
33 H. A. Barnes, *J. Non-Newtonian Fluid Mech.*, 1997, **70**(1–2), 1.
34 S. Selimovic, S. M. Maynard and Y. Hu, *J. Rheol.*, 2007, **51**(3), 325.
35 C. A. Mitchell, J. L. Bahr, S. Arepalli, J. M. Tour and R. Krishnamoorti, *Macromolecules*, 2002, **35**(23), 8825.
36 C. A. Mitchell and R. Krishnamoorti, *Macromolecules*, 2007, **40**(5), 1538.
37 E. K. Hobbie and D. J. Fry, *J. Chem. Phys.*, 2007, **126**(12).
38 V. Trappe and D. A. Weitz, *Phys. Rev. Lett.*, 2000, **85**(2), 449.